Machine Learning Based Adaptive Prediction Horizon in Finite Control Set Model Predictive Control

By

Muhammad Saleh Murtaza Gardezi

117501

Supervisor

Dr. Ammar Hasan

Department of Electrical Engineering

A thesis submitted in partial fulfillment of the requirements for the degree of Masters of Science in Electrical Engineering (MS EE)

In

School of Electrical Engineering and Computer Science,

National University of Sciences and Technology (NUST),

Islamabad, Pakistan.

(August 2017)

Approval

It is certified that the contents and form of the thesis entitled "**Machine Learning Based Adaptive Prediction Horizon in Finite Control Set Model Predictive Control**" submitted by **Muhammad Saleh Murtaza Gardezi** have been found satisfactory for the requirement of the degree.

Advisor: **Dr. Ammar Hasan**

Signature: _____

Date: _____

Committee Member 1: **Dr. Rana Iftikhar Ahmad**

Signature: _____

Date: _____

Committee Member 2: **Dr. Muhammad Latif Anjum**

Signature: _____

Date: _____

Committee Member 3: **Mr. Ahsan Azhar**

Signature: _____

Date: _____

Abstract

In this thesis, an adaptive prediction horizon approach based on machine learning is presented for the finite control set model predictive control (FCS-MPC) of power converters. Normally, in FCS-MPC, the prediction horizon (N) is fixed during both the transients and the steady-state. A large N improves performance while significantly increasing the computational cost. A novel technique is presented where the prediction horizon (N) adapts to the instantaneous states i.e. i_l, v_o and $v_{o,err} = (v_{ref} - v_o)$. Simulations are run for different combinations of N, i_l, v_o and v_{ref} to create a data set of the optimal N against the instantaneous states and the error between the reference output voltage and the output voltage and an artificial neural network is trained to tell the optimal length of N. The proposed method is simulated on a boost converter in Simulink. The simulation results show that the computational cost is reduced without affecting the performance.

Dedication

I dedicate this thesis to my father.

Certificate of Originality

I hereby declare that this submission is my own work and to the best of my knowledge it contains no materials previously published or written by another person, nor material which to a substantial extent has been accepted for the award of any degree or diploma at NUST SEECS or at any other educational institute, except where due acknowledgement has been made in the thesis. Any contribution made to the research by others, with whom I have worked at NUST SEECS or elsewhere, is explicitly acknowledged in the thesis.

I also declare that the intellectual content of this thesis is the product of my own work, except for the assistance from others in the project's design and conception or in style, presentation and linguistics which has been acknowledged.

Author Name: **Muhammad Saleh Murtaza Gardezi**

Signature: _____

Acknowledgment

I would like to thank my advisor Dr. Ammar Hasan for his invaluable guidance and extension of every possible help, my thesis committee members for being such great mentors and my family for their prayers and being behind me in difficult phases.

Table of Contents

1 Introduction **1**

1.1 Background and Motivation 1

1.2 Problem Statement 2

1.3 Proposed Method 3

2 Literature Review **4**

2.1 Digital Control Strategies 4

2.2 Finite Control Set Model Predictive Control (FCS-MPC) . . . 5

2.3 Move Blocking Strategy 6

2.4 Sphere Decoding Algorithm 6

2.5 Cyber-Physical Systems 6

3 Model of the Boost Converter **8**

3.1 Continuous-Time Model 9

3.2 Discontinuous-Time Model 11

4 Finite Control Set Model Predictive Control **14**

4.1 Objective Function 14

4.2 Optimization Problem 15

4.3 Significance of Large N 16

4.4 Move Blocking Strategy 17

4.5 Changes in Load 21

5 Proposed Adaptive Prediction Horizon 23

5.1 Cyber-physical Cost Function 23

5.2 Data Collection 25

5.3 Training 25

5.4 FCS-MPC with Adaptive Prediction Horizon 32

6 Simulation Results 35

6.1 Start-Up 36

6.2 Step Changes in the Output Reference Voltages 37

6.3 Step Change in the Input Voltage 39

6.4 Load Step Change 41

7 Conclusions 44

List of Figures

3.1 The topology of the boost converter [16]. 9
3.2 Graphical representation of the discrete modes of the boost converter [16]. 13

4.1 Non-minimum phase behaviour of the boost converter [16]. . . 17
4.2 Non-minimum phase behaviour of the boost converter with move blocking strategy [16]. 19
4.3 Prediction steps with move blocking scheme for a) output voltage, b) inductor current and c) control input. 20

5.1 A representation of an artificial neural network. 26
5.2 The start up of the neural network toolbox in MATLAB. . . . 27
5.3 Selection of input and output matrices. 28
5.4 Specify the number of hidden neurones. 29
5.5 Choose Bayesian-Regularization as the training algorithm. . . 30
5.6 Training starts and stops when either 1000 iterations are complete or the mean squared error stops decreasing. 31
5.7 Form the function 'adapt' which chooses the optimal N. 32
5.8 Block diagram of FCS-MPC scheme with adaptive prediction horizon and Kalman filter. 33

6.1 A simulated start-up behaviour of output voltage, inductor current and the optimal prediction horizon. 37
6.2 The simulated behaviour of output voltage, inductor current and the optimal prediction horizon for a step-down change in output reference voltage. 38
6.3 The simulated behaviour of output voltage, inductor current and the optimal prediction horizon for a step-up change in output reference voltage. 39
6.4 The simulated behaviour of output voltage for a step-up change in input voltage. 40
6.5 The simulated behaviour of inductor current for a step-up change in input voltage. 41
6.6 The simulated behaviour of output voltage for a change in load. 42
6.7 The simulated behaviour of the prediction horizon for a change in load. 43

Chapter 1

Introduction

1.1 Background and Motivation

Model predictive control (MPC) uses a discrete-time model of the system to "predict" the future values of the system based on the current state. In power electronic converters, the control input is the on/off actuation of the switch. This entails that the possible inputs are finite in number. This variant of MPC is called the finite control set model predictive control (FCS-MPC). The finite number of possible inputs produce a finite number of possible switching sequences. The number of prediction steps in the horizon (N) dictates the length of the switching sequences and thus, tells how far ahead we "see" in the future. A cost function is defined and FCS-MPC solves an optimization problem for every sequence. The sequence that minimizes the cost function is the optimal sequence. The optimization problem is solved online at every sampling instant and the first actuation of the sequence is then applied to the converter. This process is repeated at every time step for new state values and is known as receding horizon policy [18].

The main disadvantage of the MPC is the large computational cost asso-

ciated. The time intervals in power electronic converters are in the microseconds and in real-time, the optimization problem is computationally extensive to solve. The prediction horizon is an important factor in MPC. A larger prediction horizon increases the performances of the system [24] but at the same time, increases the computational cost as the number of sequences to be searched increase exponentially. Moreover, the power electronic converters that exhibit a non-minimum phase behaviour require a large prediction horizon for stability.

The computational cost of MPC could be reduced if the prediction horizon was varying. A trade off between the physical performance and the cyber performance (computational cost) could be achieved similar to a cyber-physical system [1, 7]. A cyber-physical system (CPS) consists of both the physical as well as the cyber aspect of the system. A CPS approach to the attitude control of the CubeSat satellite is presented in [2]. Due to the limitation of resources in the satellite, the computational power is shared by all tasks being carried out. The controller regulates both the physical and cyber resources of the satellite. Similarly, a cyber-physical cost function (J_{cp}) can be defined for an FCS-MPC controlled converter that contains information of both the cyber utilization and physical performance of the converter.

1.2 Problem Statement

The solutions to the computational complexity of MPC that exist all focus on solving the optimization problem efficiently. However, none of the solutions that exist talk about the cyber-physical aspect of MPC. A larger prediction horizon improves performance while simultaneously, posing a high computational cost. Therefore, a cyber-physical function for MPC has to be formed

that provides a trade off between the physical performance and the cyber utilization. This would allow the prediction horizon to be smaller and thus, reducing the computational complexity.

1.3 Proposed Method

A novel technique is proposed where the prediction horizon (N) is always varying instead of being fixed. An artificial neural network tells what N to choose at run-time. Several simulations were run with different conditions of converter states i.e. il, vo and $v_{o,err}$ for a range of N and the resulting cyber-physical cost (J_{cp}) was determined. For the different conditions of converter states, that particular N from the range was assigned that registered the smallest J_{cp}. A data set of these states and the corresponding N is created. An artificial neural network was trained on the data set to learn the behaviour and predict the optimal N at run-time.

The proposed method is applied on a boost converter. The main objective of the controller is to regulate the output voltage to a set reference. A discrete-time model for the boost converter is determined that incorporates both the continuous conduction mode (CCM) and the discontinuous conduction mode (DCM). A discrete Kalman filter [23] is included with the control scheme to cater for the changes in load and provide an offset-free voltage regulation.

Chapter 2

Literature Review

2.1 Digital Control Strategies

In recent years, the applications of dc-dc converters have widened, ranging from dc power supplies, dc motor control [11], electric vehicles, hybrid electrical systems and renewable energy systems. With the dc-dc converters comes the need to control the converters to desired conditions. In this aspect, linear control techniques like pulse-width-modulation and PI [6] have been applied on power converters. However, the control techniques pose problems such as extensive manual tuning.

Ever since the dawn of fast processors, researchers have been able to come up with newer control techniques that are superior to the classical control. Embedded systems and digital processors have enabled the use of techniques like feedforward control [8,9], fuzzy logic [13,22], nonlinear techniques [5,21], sliding mode [14, 19] and H_∞ [10]. One of the control method that takes advantage of the processing power is the model predictive control (MPC) [20] that eliminates the manual tuning of the controller.

2.2 Finite Control Set Model Predictive Control (FCS-MPC)

Model predictive control (MPC) uses a discrete-time model of the system to "predict" the future values of the system based on the current state. In power electronic converters, the control input is the on/off actuation of the switch. This entails that the possible inputs are finite in number. This variant of MPC is called the finite control set model predictive control (FCS-MPC). The finite number of possible inputs produce a finite number of possible switching sequences. The number of prediction steps in the horizon (N) dictates the length of the switching sequences and thus, tells how far ahead we "see" in the future. A cost function is defined and FCS-MPC solves an optimization problem for every sequence. The sequence that minimizes the cost function is the optimal sequence. The optimization problem is solved online at every sampling instant and the first actuation of the sequence is then applied to the converter. This process is repeated at every time step for new state values and is known as receding horizon policy [18].

The main disadvantage of the MPC is the large computational cost associated. The time intervals in power electronic converters are in the microseconds and in real-time, the optimization problem is computationally extensive to solve. The prediction horizon is an important factor in MPC. A larger prediction horizon increases the performances of the system [24] but at the same time, increases the computational cost as the number of sequences to be searched increase exponentially. Moreover, the power electronic converters that exhibit a non-minimum phase behaviour require a large prediction horizon for stability.

2.3 Move Blocking Strategy

Move-blocking scheme [16, 17] was introduced in MPC by breaking the horizon into fine and coarse time steps. For the immediate future, fine time intervals were used while coarse time intervals were used for the future far ahead. This meant that the states of the converter could be "predicted" further ahead by applying a comparatively smaller N that reduced the computational complexity.

2.4 Sphere Decoding Algorithm

Instead of exhaustive search, one solution is to reduce the computational cost by efficiently solving the optimization problem. Techniques like sphere decoding [4] were introduced in the realm of MPC to replace the exhaustive search with solving the optimization problem in a vector form. This converts the optimization problem to an integer least square problem. Thus, the optimal switching position is found in a more cost-effective manner. However, this technique is suitable for multilevel inverters and present complexities in its application to dc-dc converters. Other efficient solutions to FCS-MPC involve techniques like event-based horizon and extrapolation strategy [12].

2.5 Cyber-Physical Systems

The techniques explained in previous sections have a fixed number of prediction steps N in the horizon. The computational cost of MPC could be reduced if the prediction horizon was varying. A trade off between the physical performance and the cyber performance (computational cost) could be achieved similar to a cyber-physical system [1, 7]. A cyber-physical system

(CPS) consists of both the physical as well as the cyber aspect of the system. A CPS approach to the attitude control of the CubeSat satellite is presented in [2]. Due to the limitation of resources in the satellite, the computational power is shared by all tasks being carried out. The controller regulates both the physical and cyber resources of the satellite. Similarly, a cyber-physical cost function (J_{cp}) can be defined for an FCS-MPC controlled converter that contains information of both the cyber utilization and physical performance of the converter.

Chapter 3

Model of the Boost Converter

The topology of the boost converter is shown in Fig. 3.1. A boost converter increases the output voltage of the system to higher value than the voltage supplied to the converter. The inductor (L) charges itself initially to store current which is then used to charge the capacitor (C_o) to the desired value of the output voltage. Moreover, the inductor also functions to reduce the ripple in the inductor and the output capacitor reduces the ripples in the output voltage. After the initial charging of the inductor and the capacitor, the switch (S) is applied with actuation inputs to regulate the output voltage to the reference voltage. The parasitic resistance of the inductor is denoted by R_L

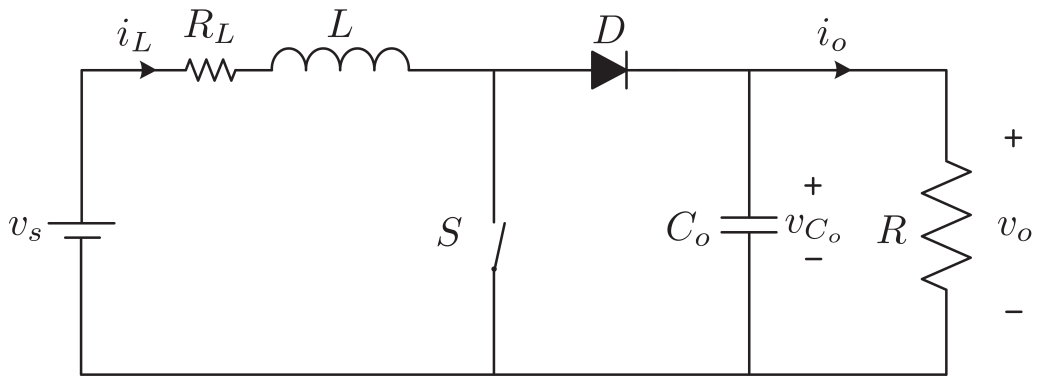

Figure 3.1: The topology of the boost converter [16].

3.1 Continuous-Time Model

The continuous model of the boost converter should incorporate the three modes of operations of the boost converter.

1. The switch (S) is ON and the diode (D) is OFF
2. The switch (S) is OFF and the diode (D) is ON
3. The switch (S) is OFF and the inductor current $i_l = 0$, which turns OFF the diode (D)

In mode 1, the inductor is storing current and at the same time, not letting the current to fall. However, the output voltage falls. In mode 2, the inductor releases its stored current to charge the output capacitor (C_o) which causes the rise of output voltage across the load (R). This process happens quite rapidly that only a small ripple is observed in the current and voltage. These two modes are the continuous conduction mode (CCM) since the inductor current is greater than zero. However, the converter goes in

mode 3 when the inductor current $i_l = 0$. This cause the diode to switch off. This is the discontinuous conduction mode (DCM).

The state-space model of the boost converter for continuous-time is given as [3]:

$$dx(t)/dt = (A_1 + A_2 u(t))x(t) + Bv_s(t) \tag{3.1a}$$

$$y(t) = Cx(t) \tag{3.1b}$$

where

$$x(t) = \begin{bmatrix} i_l(t) & v_o(t) \end{bmatrix}^T \tag{3.2}$$

is the state vector, v_s is the input voltage, u(t) is the input applied to the switch (S) i.e. either 0 meaning the switch (S) is OFF or 1 meaning the switch (S) is ON and

$$A_1 = \begin{bmatrix} -\frac{d_{aux}R_L}{L} & -\frac{d_{aux}}{L} \\ \frac{d_{aux}}{C_o} & -\frac{1}{C_oR} \end{bmatrix}, \quad A_2 = \begin{bmatrix} 0 & \frac{1}{L} \\ -\frac{1}{C_o} & 0 \end{bmatrix}, \quad B = \begin{bmatrix} \frac{d_{aux}}{L} & 0 \end{bmatrix}^T$$

$$\text{and} \quad C = \begin{bmatrix} 0 & 1 \end{bmatrix}$$

d_{aux} can take the value of either 0 or 1 and determines whether the converter operates in CCM or DCM. d_{aux} takes the value 1 if the converter is operating in continuous conduction mode (CCM) and a value of 0 is assigned to d_{aux} if the converter is operating in discontinuous conduction mode (DCM). The mathematical expression to explain this is given as:

$$d_{aux}(t) = \begin{cases} 1 & \text{if } u(t) = 1, \text{or } u(t) = 0 \text{ and } i_l(t) > 0 \\ 0 & \text{if } u(t) = 0 \text{ and } i_l(t) = 0 \end{cases} \tag{3.3}$$

3.2 Discontinuous-Time Model

Model predictive control (MPC) uses the discrete-time model to "predict" the future values of the converter. Therefore, an accurate discrete-time model that incorporates all modes of operation is need. This requires the conversion of continuous-time model matrices to discrete-time model matrices. We denote these discrete models as follows:

$$\Gamma_1 = A_1 \text{ for } d_{aux} = 1$$

$$\Gamma_2 = A_1 \text{ for } d_{aux} = 0$$

$$\Gamma_3 = A_2, \text{ and}$$

$$\Delta = B \text{ for } d_{aux} = 1$$

By using the continuous-time model from equation (3.1) and Euler's approximation, the following discrete-time model for the boost converter with a sampling interval, T_s, is obtained [16]:

$$x(k+1) = \begin{cases} E_1 x(k) + F_1 v_s(k) & \text{Mode 1} \\ E_2 x(k) + F_2 v_s(k) & \text{Mode 2} \\ E_3 x(k) + F_3 v_s(k) & \text{Mode 3} \\ E_4 x(k) & \text{Mode 4} \end{cases} \tag{3.5a}$$

$$y(k) = Gx(k) \tag{3.5b}$$

where the matrices are defined as:

$$E_1 = \mathbf{1} + (\Gamma_1 + \Gamma_3)$$

$$E_2 = \mathbf{1} + \Gamma_1 T_s$$

$$E_3 = \frac{1}{2}(E_1 + E_2)$$

$$E_4 = \mathbf{1} + \Gamma_2 T_s$$

$$F_1 = \Delta T_s$$

$$F_2 = F_1$$

$$F_3 = \frac{1}{2}\Delta, \text{ and}$$

$$G = C$$

$\mathbf{1}$ is an identity matrix of order 2. The graphical representation of the discrete modes of the boost converter is illustrated in Fig. 3.2.

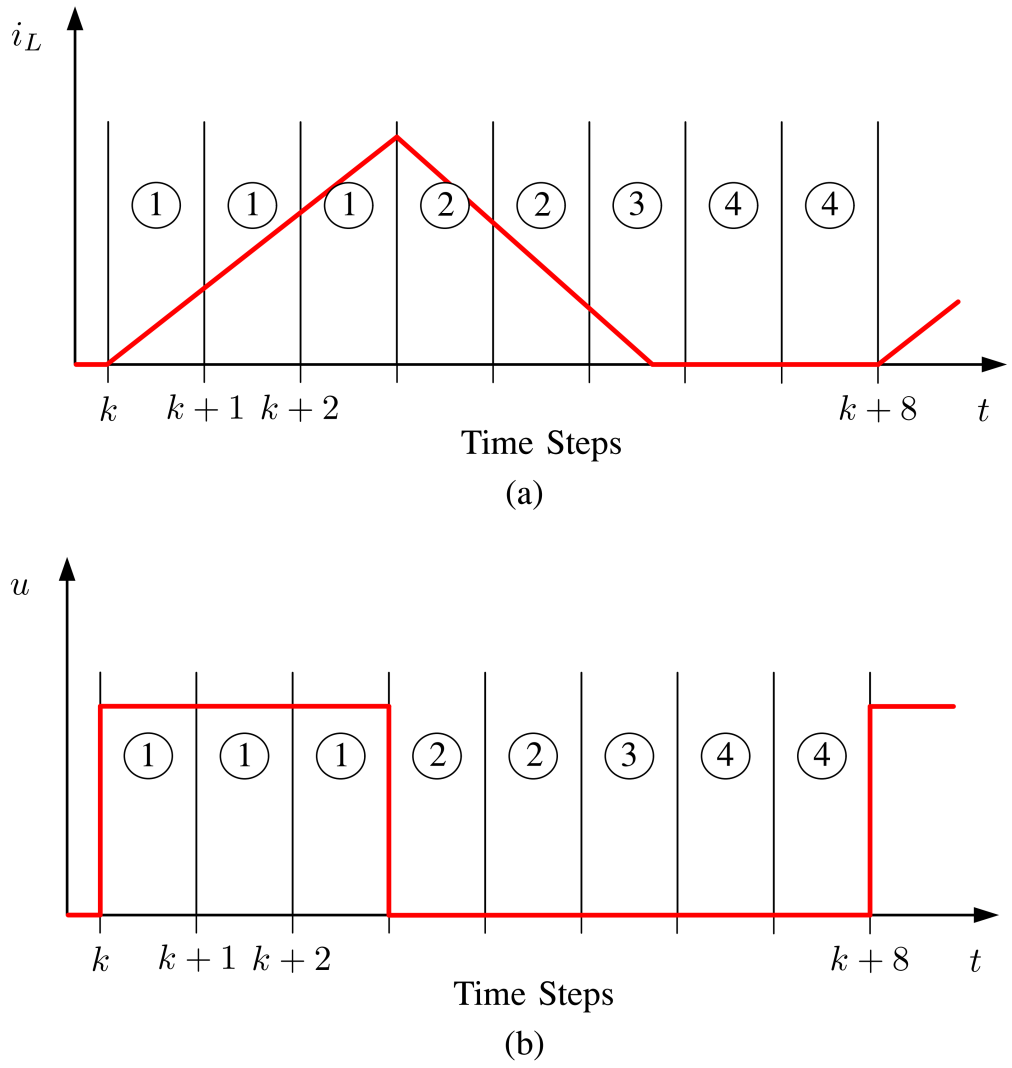

Figure 3.2: Graphical representation of the discrete modes of the boost converter [16].

Chapter 4

Finite Control Set Model Predictive Control

Finite control set refers to the finite number of actuation sequences that occur for a fixed number of prediction steps in the horizon. All possible control sequences are first determined and then, model predictive control solves the optimization problem for all sequences in the control set and chooses the sequences that has the lowest cost.

4.1 Objective Function

The objective function opted is:

$$J = \sum_{l=k}^{k+N-1} |v_{ref} - v_o(l)| + \lambda |u(l-1) - u(l)| \tag{4.1}$$

where N is the number of prediction steps in the horizon over which the variables of interest are penalized. N is a finite number. v_{ref} is the reference voltage which the output voltage should track while u represents the switch

being either on or off. The first term in the objective function penalizes the error between the reference output voltage and the output voltage.

$$v_{o,err} = v_{ref} - v_o(k) \tag{4.2}$$

The second term of the objective function is the difference between the previous switching state and the current switching state. This prevents the excessive switching and reduce the switching frequency of the switch.

$$\Delta u(k) = u(k-1) - u(k) \tag{4.3}$$

The term λ is the weighting factor and decides the bias of the objective function. It is usually set to a smaller value because the bias tends towards reducing the error between the reference output voltage and the output voltage.

4.2 Optimization Problem

The optimization problem is to minimize the objective function posed in (4.1).

$$U^*(k) = \arg\min J(k) \text{subject to equation (3.5)} \tag{4.4}$$

The solution of the optimization problem is a sequence of the form:

$$U(k) = [u(k)u(k+1)u(k+2)...u(k+N-1)]$$

The sequence that provides the lowest value of $J(k)$ is the optimal sequence and is denoted by $U^*(k)$. However, only the first entry of the optimal sequence, $u^*(k)$, is applied as input to the converter switch. This optimization problem is solved online at every time step.

The solution to this optimization problem is a tricky one because it is a mixed integer nonlinear optimization problem. Note that modes 1 and 2 are affine (linear plus offset), mode 3 is nonlinear and mode 4 is linear. The simplest solution to this problem is the use of enumeration or exhaustive search. First, all possible sequences are defined for the prediction horizon which are 2^N in number. For each sequence, the cost of objective function is found and the sequence that has the lowest cost is the optimal sequence. However, this method is not very computationally efficient as the cost of 2^N sequences has to be found in the sampling interval, T_s.

4.3 Significance of Large N

The boost converter exhibits a non-minimum phase behavior (shown in Fig. 4.1) that entails an initial drop in the output voltage when the reference voltage is increased. This attitude requires a prediction horizon large enough to "see" the eventual rise of output voltage after it drops. The move-blocking strategy [16] was devised for a seemingly large N with the computational cost of a smaller prediction horizon. Furthermore, a large prediction horizon also improves the physical performance of the converter [24] in the transient state where it helps to reach the reference voltage in a shorter time.

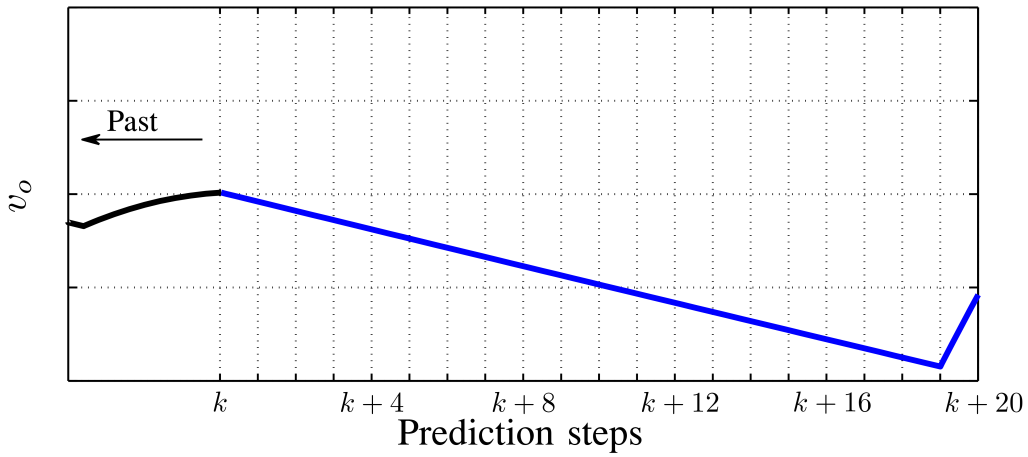

Figure 4.1: Non-minimum phase behaviour of the boost converter [16].

4.4 Move Blocking Strategy

As discussed in the previous section, the main issue presented by the boost converter for its voltage control is that it poses a non-minimum phase behaviour. This means that when the reference voltage to be tracked is increased, the output voltage drops at first. This is because during this time, the inductor is charging up to eventually charge up the output capacitor. Therefore, the prediction horizon should be large enough to "see" the eventual rise of the output voltage to maintain the stability of the converter.

To avoid the loss of stability of the converter, NT_s should be large enough. However, increasing N would increase the number of computations because the number of control sequence would increase while increasing T_s would decrease the resolution of the measurements. Both cases are not beneficial for the cause. This is where move blocking comes in. Move blocking breaks the prediction intervals into fine and coarse samples as shown in the equation below

$$N_1 T_s + N_2 n_s T_s$$

where n_s is a constant multiplying factor that increases the sampling time further ahead in the future. The resolution of measurements do not affect the control in the future because only the measurements in the near future are of importance. If a prediction horizon of 20 is used, the total prediction interval is $20T_s$. However, with move blocking

$$N = N_1 + N_2$$

$$\text{If } N_1 = 7 \text{ and } N_2 = 4$$

$$\text{then } N = 11$$

$$\text{the total prediction interval if } n_s = 4 \text{ is}$$

$$N_1 T_s + N_2 n_s T_s = 23Ts$$

As demonstrated by the equations above and Fig. 4.2, a prediction horizon of 11 with move blocking strategy provides more prediction steps than a prediction horizon of 20 without move blocking strategy.

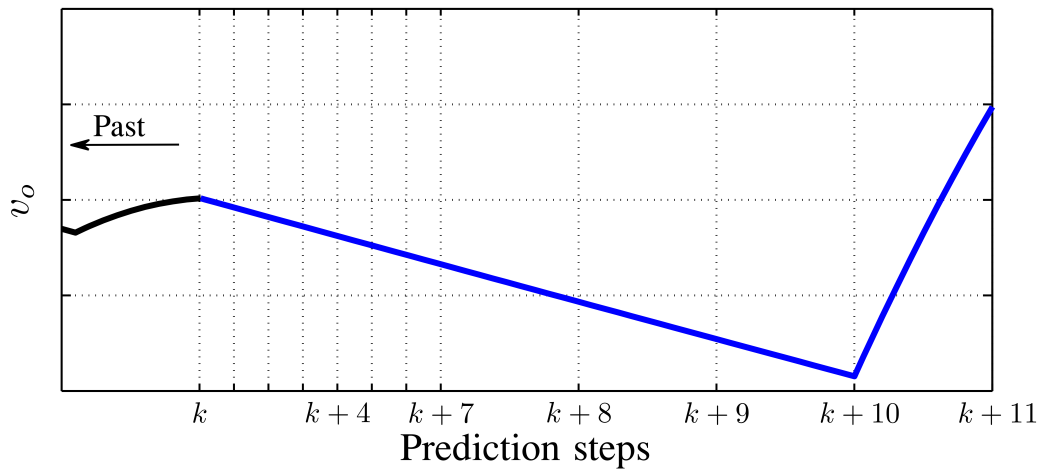

Figure 4.2: Non-minimum phase behaviour of the boost converter with move blocking strategy [16].

It should also be noted that the number of possible control sequences for a prediction horizon of 20 without move blocking strategy amounts to:

$$2^N = 2^{20} = 1048576$$

while the number of possible control sequences for a prediction horizon of 11 with move blocking strategy amounts to:

$$2^N = 2^{11} = 2048$$

These numbers indicate a decrease of 99.9% in the number of computations. Moreover, increasing the prediction horizon increases the number of possible sequences and thus, the computational cost exponentially.

Another point to be noted is that fine time steps are only required in the near future and coarse time steps are enough for the future further ahead. This is because of the receding horizon policy implemented in the model predictive control (MPC). As the time increases step by step, the once coarse

time samples are converted to fine time samples. The behaviour of the boost converter is illustrated in Fig. 4.3.

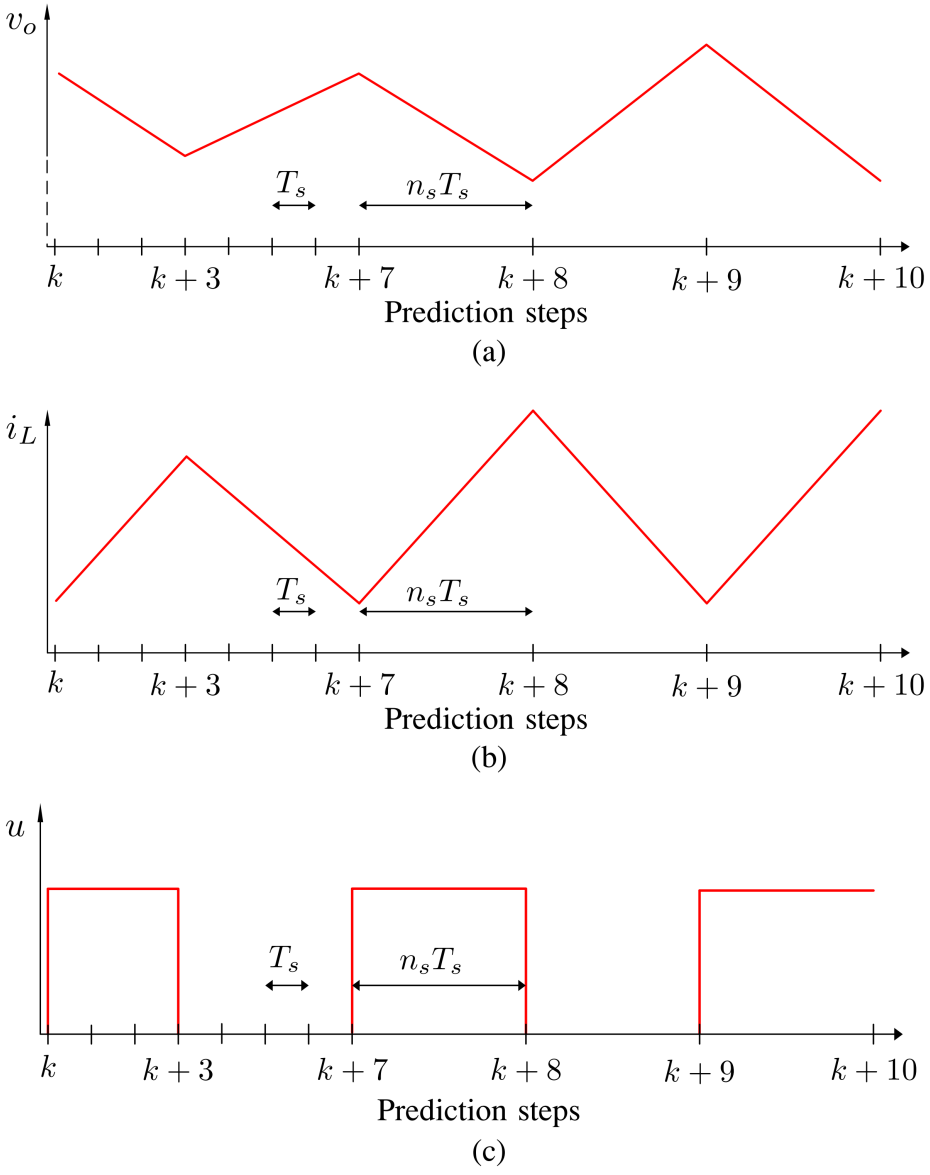

Figure 4.3: Prediction steps with move blocking scheme for a) output voltage, b) inductor current and c) control input.

4.5 Changes in Load

The load is often time-varying and unknown in most applications. Thus, a Kalman filter [15, 16] is added to the control scheme to provide offset-free tracking of the reference voltage during changes in load as presented in. In addition to the measured states, i_l and v_o, disturbance states i_e and v_e are added to form an augmented state vector

$$x_a = \begin{bmatrix} i_l & v_o & i_e & v_e \end{bmatrix}^T \tag{4.5}$$

Therefore, the state space model changes to

$$x_a(k+1) = E_{aM}x(k) + F_{aM}v_s(k) \tag{4.6a}$$

$$y_a(k) = G_a x(k) \tag{4.6b}$$

$$E_{aM} = \begin{bmatrix} E_M & \mathbf{0} \\ \mathbf{0} & \mathbf{1} \end{bmatrix}, F_{aM} = \begin{bmatrix} F_M \\ 0 \\ 0 \end{bmatrix} \text{ and } \quad G_a = \begin{bmatrix} \mathbf{1} & \mathbf{1} \end{bmatrix} \tag{4.7}$$

where $\mathbf{1}$ and $\mathbf{0}$ are identity matrix and a null matrix of order two respectively.

A discrete Kalman filter is designed with four different Kalman gains K_M according to the mode of operation. The noise covariance matrices Q and R are assigned such that high credibility is associated with the measured state while the disturbance states have low credibility associated with them. Thus, the estimated state equation is defined as

$$\hat{x}(k+1) = E_{aM}\hat{x}_a(k) + K_M G_a(\hat{x}_a(k))F_{aM}v_s(k) \tag{4.8}$$

The estimated disturbance state is used to eliminate the offset from the reference by altering the reference voltage to

$$\hat{v}_{ref} = v_o - \hat{v}_e \tag{4.9}$$

Instead of the measured states, i_l and v_o, the estimated states $\hat{i}_l$ and $\hat{v}_o$ are used as input vector to the controller.

Chapter 5

Proposed Adaptive Prediction Horizon

In the standard FCS-MPC scheme [16], the prediction horizon is fixed. An increase in prediction horizon improves the physical performance but the computational complexity also increases. The purpose of the proposed method is to find a prediction horizon that provides a trade off between great physical performance and low computational complexity. However, a fixed prediction horizon that provides this trade off will not suffice. A prediction horizon that adapts itself to the changing values of i_l, v_o and $v_{o,err}$ during disturbances in load, changes in output reference voltage, transients and steady-state is needed. The proposed method of determining the adaptive prediction horizon is explained in the following subsections.

5.1 Cyber-physical Cost Function

A cyber-physical cost function is defined as a metric to determine the effect of different number of prediction steps in the horizon N on the physical

performance of the converter and the cyber resource utilization. It is the sum of the physical performance, J_p and the weighted cyber utilization, J_c.

$$J_p := \sum_{k=1}^{M} |v_{ref} - v_o(l)| + \lambda |u(l-1) - u(l)| \tag{5.1a}$$

where λ is a weighting factor similar to equation (2) and M is the number of samples to assess the physical performance. M is a fixed arbitrary number and should be set sufficiently greater than the number of prediction steps in the horizon, N. In the proposed method, its value is $M = 100$ which entails that J_p contains the information of the physical performance for 100 samples.

The cyber utilization is defined as

$$J_c := 2^N \tag{5.1b}$$

and the cyber-physical cost function is

$$J_{cp} := J_p + \gamma J_c \tag{5.1c}$$

where γ is a constant less than one used adjust the value of the cyber-physical cost since J_c tends to have a rather large value.

It can be seen from (8a) that J_p is an accumulation of the error for 100 time steps. In case of large N, the term $(v_{ref} - v_o)$ gets smaller quite quickly because of increased performance resulting in a smaller value of J_p which is desirable but at the same time, the value of J_c is large because of greater resource utilization. Thus, a trade off has to be found between the physical performance and the cyber utilization.

5.2 Data Collection

A range of values for N, i_l, v_o and $v_{o,err}$ are defined. For every possible combination of N, i_l, v_o and $v_{o,err}$, simulations are run and the corresponding J_p is determined. The values of v_o for $M = 100$ samples to determine J_p are calculated by the MPC algorithm with move blocking presented in [16]. For every possible combination of values of i_l, v_o and $v_{o,err}$, the corresponding N is chosen which has the smallest value of J_{cp}. A training data set is formed using this strategy where an optimal number of prediction steps in the horizon, N_o, is related to every combination of i_l, v_o and $v_{o,err}$.

5.3 Training

The artificial neural network is a supervised machine learning technique that is analogous to function mapping. It is inspired by the biological neural network where several nodes combine themselves in a network to relate several features or inputs to an output. In the proposed case, the inputs are the states of the converter ,i_l and v_o, and the error between the reference voltage and output voltage, $v_{o,err}$, which outputs the prediction horizon N to be chosen for the particular states.

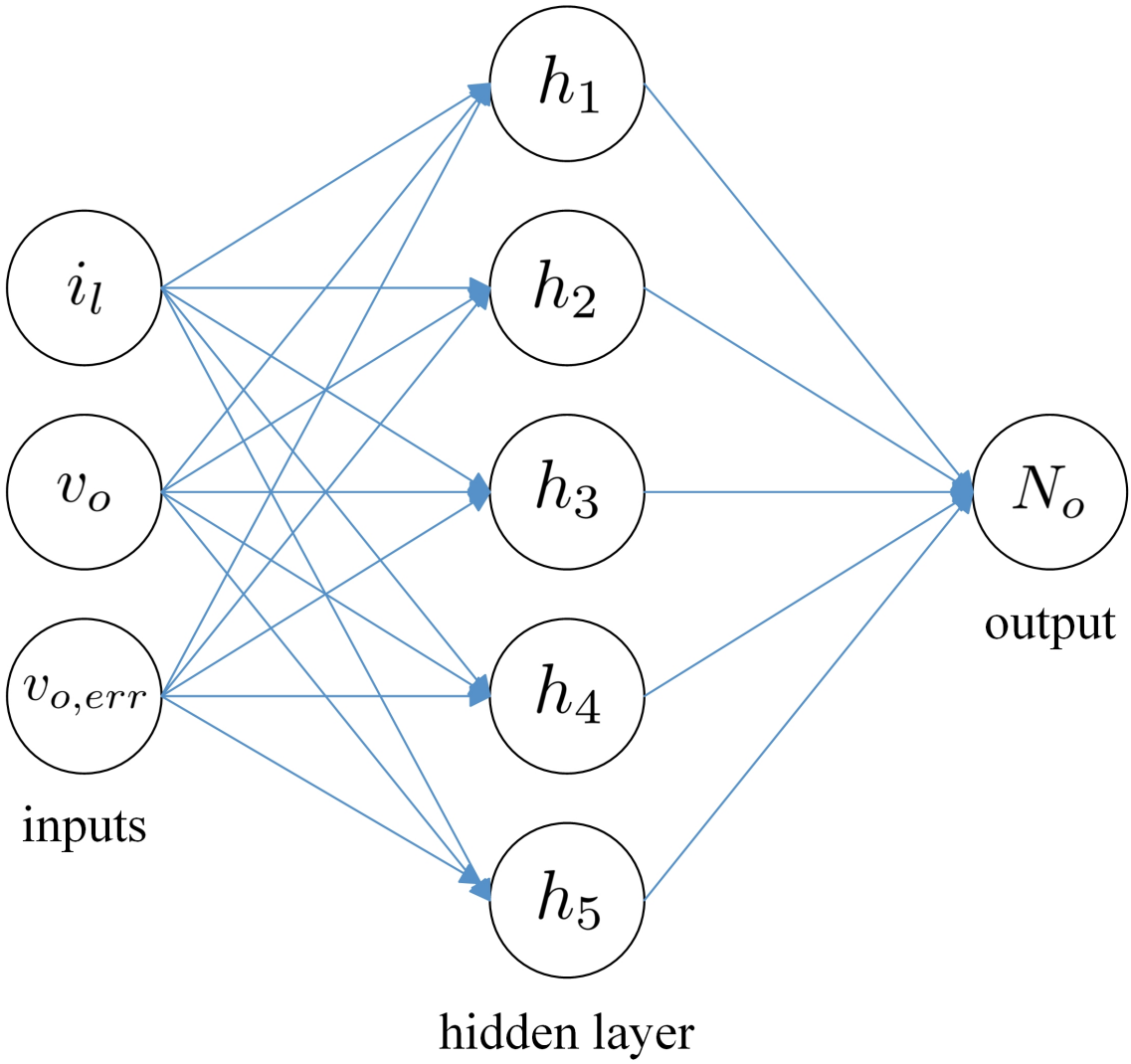

Figure 5.1: A representation of an artificial neural network.

For the training data set formed, an artificial neural network is trained to learn the relation between the inputs and the output. For the proposed method, an artificial neural network toolbox based on Bayesian Regularization in MATLAB was used to train the artificial neural network. The trained neural network forms a function that takes i_l, v_o and $v_{o,err}$ as input and outputs the optimal prediction horizon, N_o.

$$N_o = adapt(i_l, v_o, v_{o,err}) \tag{5.2}$$

The data collection and training is done offline and N_o is dictated by (9) online at every sampling interval.

The steps to use the toolbox in MATLAB are illustrated in Fig. 5.2 to Fig. 5. 7.

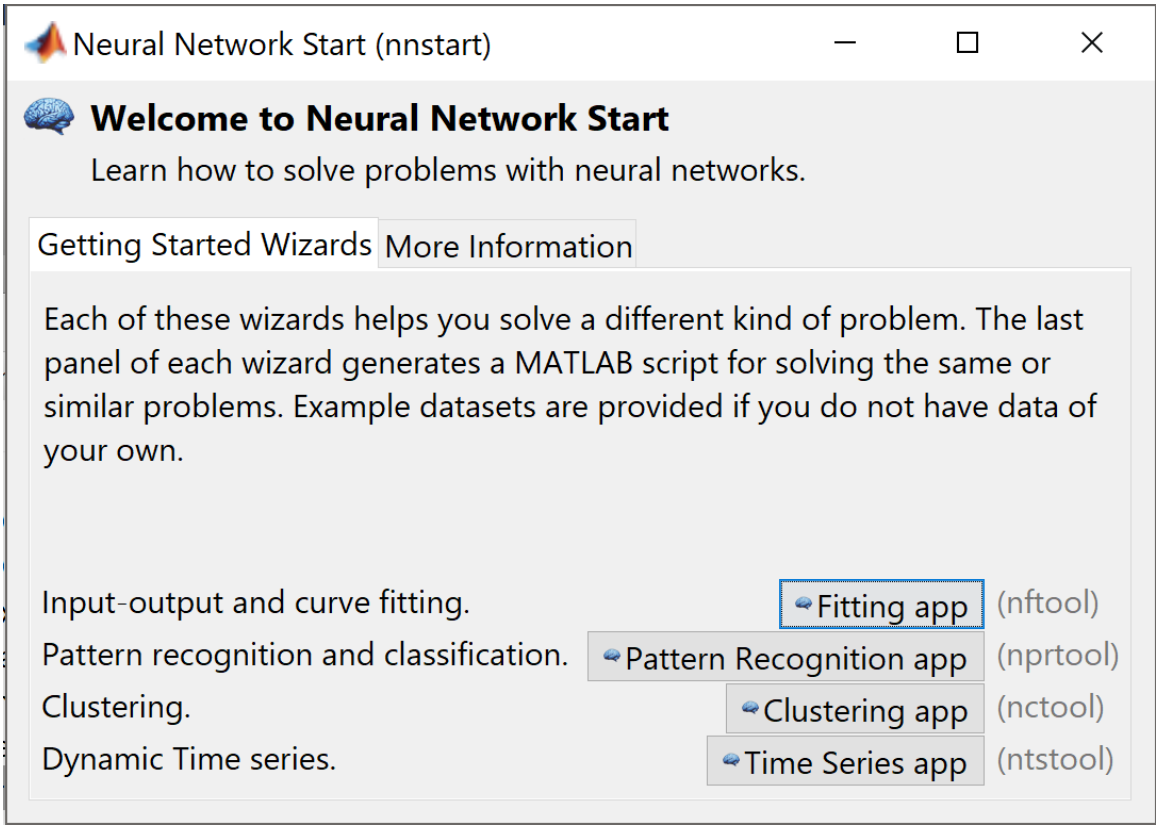

Figure 5.2: The start up of the neural network toolbox in MATLAB.

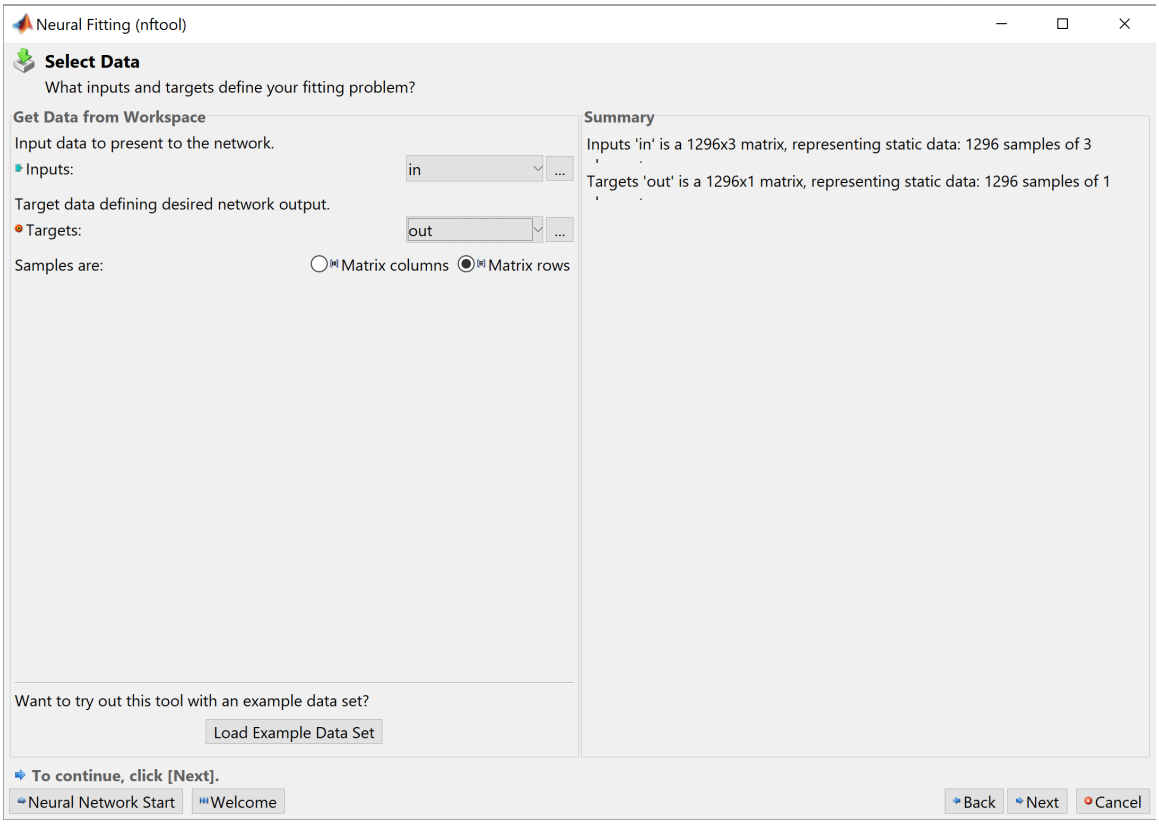

Figure 5.3: Selection of input and output matrices.

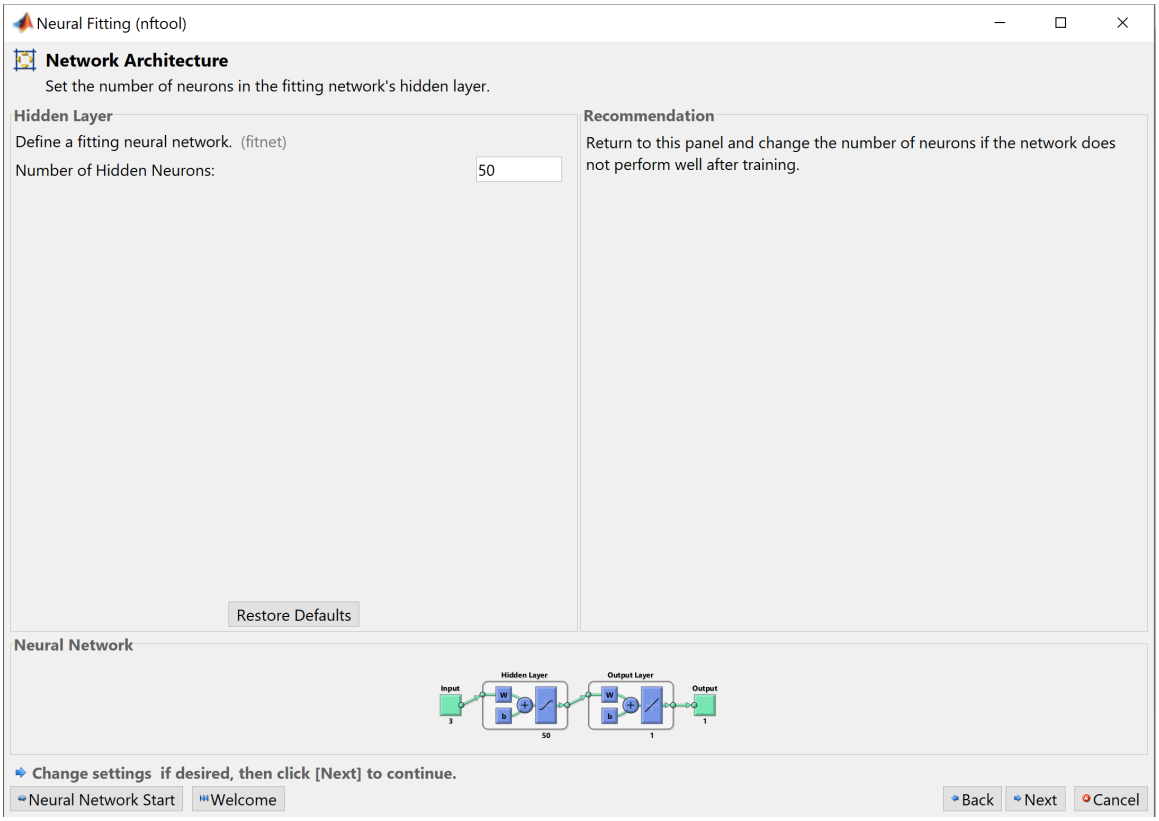

Figure 5.4: Specify the number of hidden neurones.

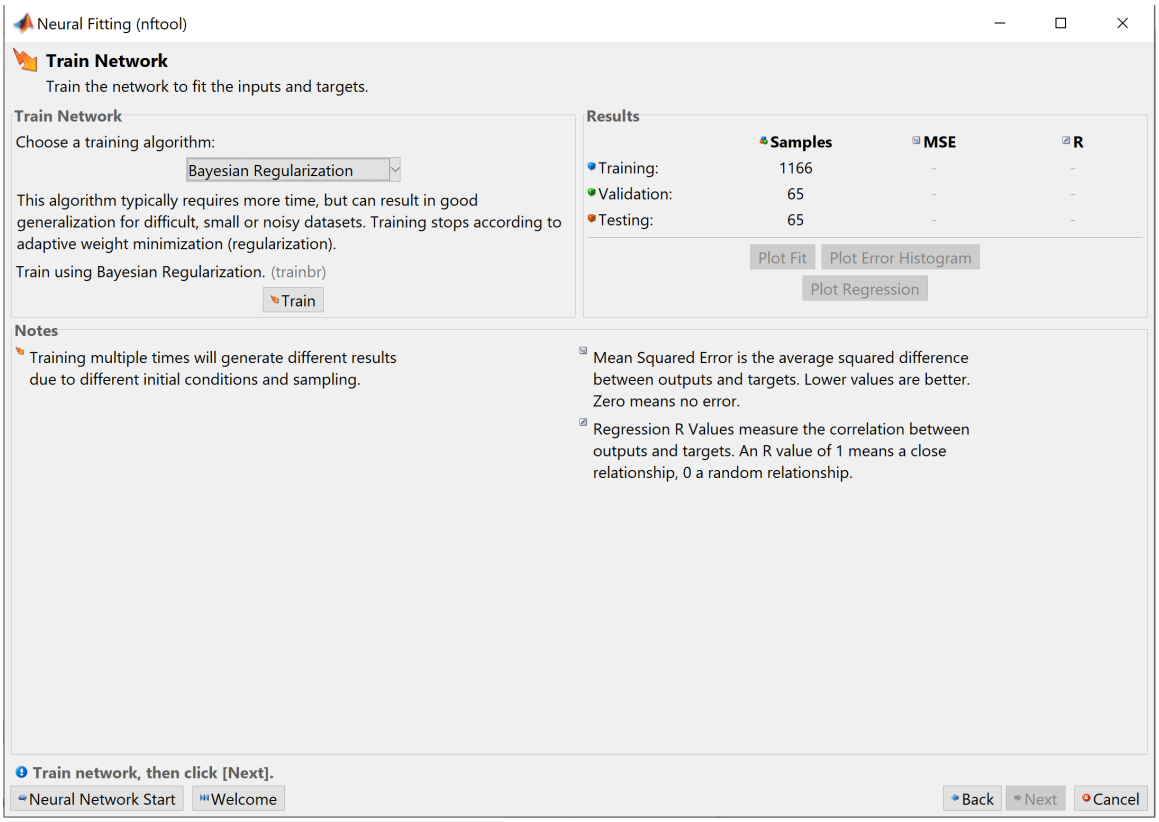

Figure 5.5: Choose Bayesian-Regularization as the training algorithm.

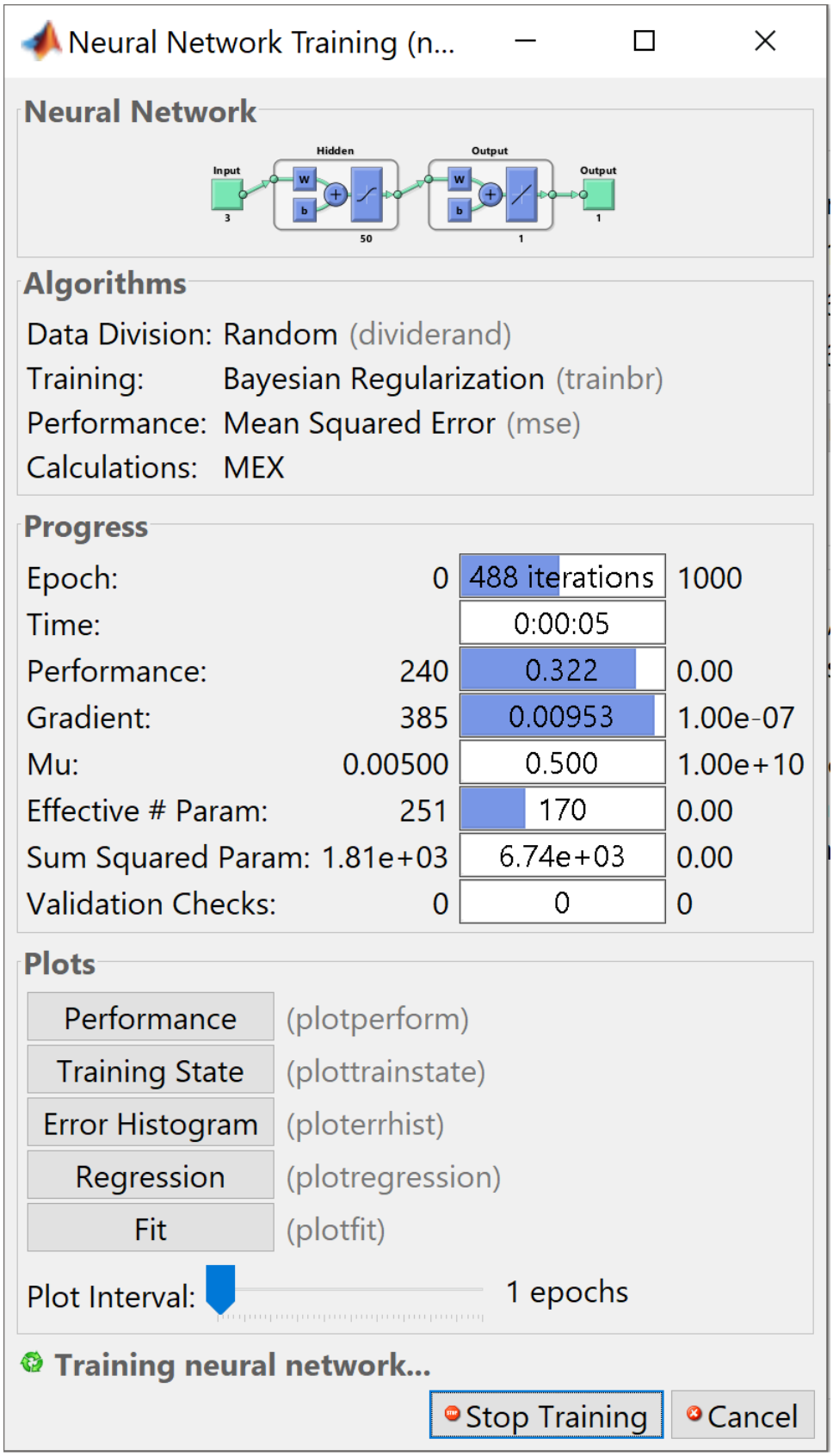

Figure 5.6: Training starts and stops when either 1000 iterations are complete or the mean squared error stops decreasing.

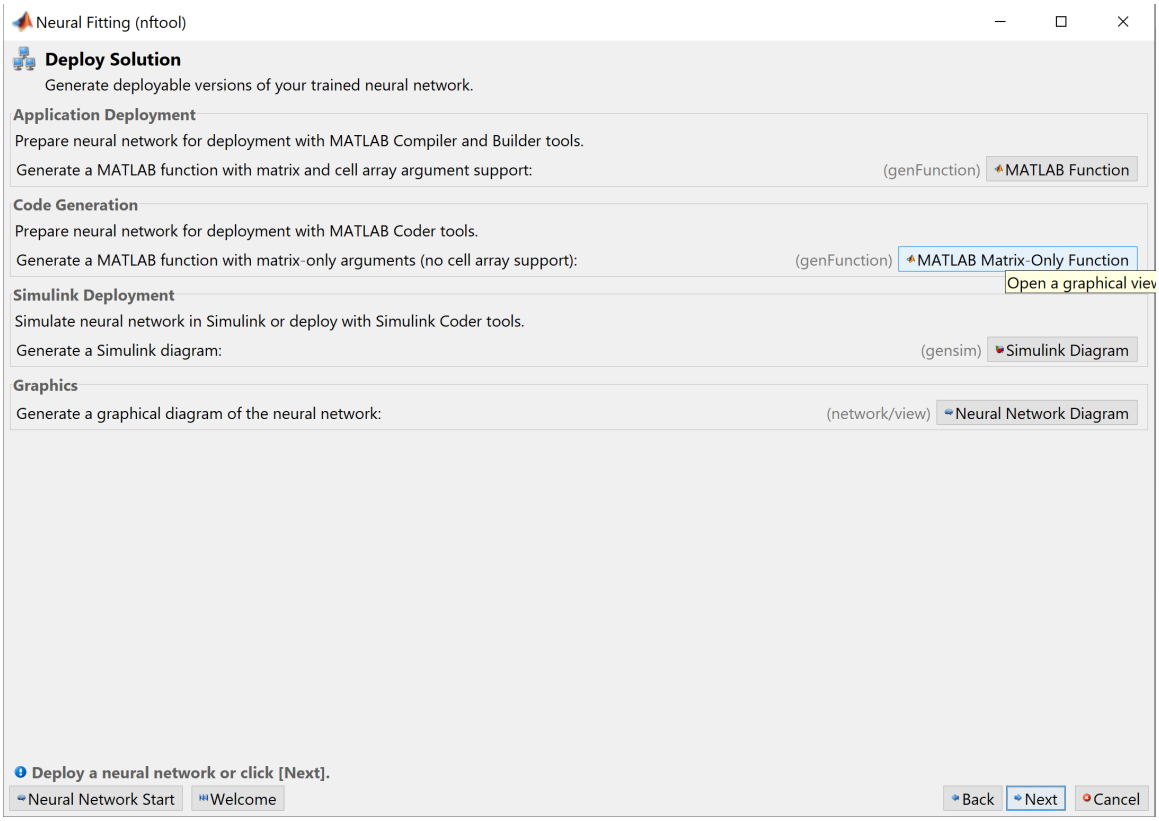

Figure 5.7: Form the function 'adapt' which chooses the optimal N.

5.4 FCS-MPC with Adaptive Prediction Horizon

The control scheme proposed is summarized in Algorithm 2. Instead of fixed prediction horizon, the algorithm adapts the horizon depending on i_l, v_o and $v_{o,err}$ and the optimal prediction horizon, N_o, is determined by (9). The function f_1 denotes a state model with fine sampling time, T_s, while f_2 denotes a state model with coarse sampling time, $n_s T_s$ The block diagram of the proposed control method is shown in Fig. 2.

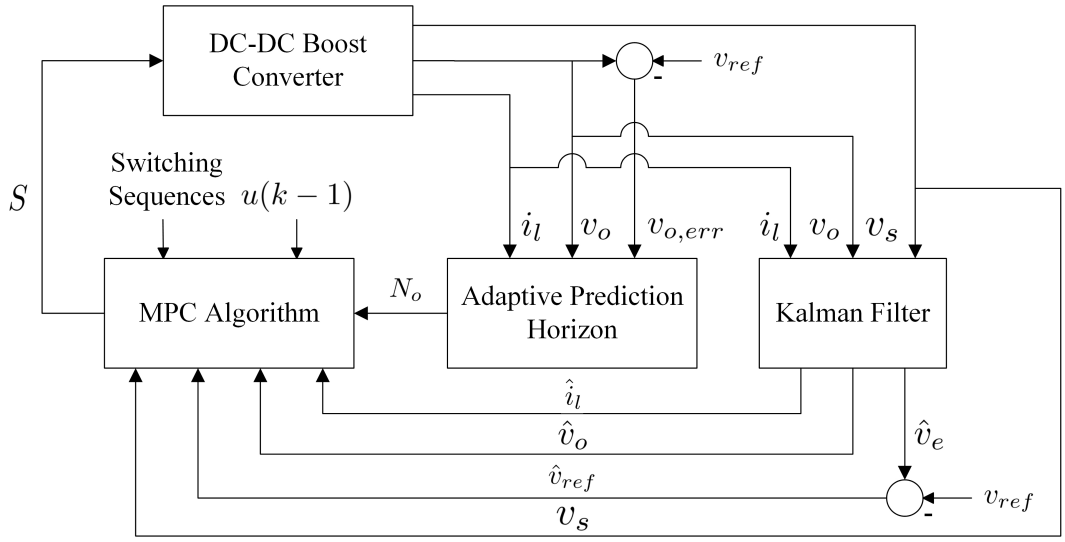

Figure 5.8: Block diagram of FCS-MPC scheme with adaptive prediction horizon and Kalman filter.

Algorithm 5.1 FCS-MPC with Adaptive Prediction Horizon

function MPC($i_l, v_o, v_{o,err}, \hat{x}(k), u(k-1)$)

$J^*(k) = \infty; u^*(k) = \emptyset; x(k) = \hat{x}(k)$

$N_o = adapt(i_l, v_o, v_{o,err})$

for all U over N_o **do**

$J = 0$

for $l = k$ to $k + N_o + 1$ **do**

if $l < k + N_1$ **then**

$x(l+1) = f_1(x(l), u(l))$

else

$x(l+1) = f_2(x(l), u(l))$

end if

$v_{err}(l+1) = \hat{v}_{ref} - v_o(l+1)$

$J = J + |v_{err}(l+1)| + \lambda|u(l) - u(l-1)|$

end for

if $J < J^*(k)$ **then**

$J^*(k) = J$

$u^*(k) = U(1)$

end if

end for

end function

Chapter 6

Simulation Results

The simulation results of the proposed control scheme with adaptive prediction horizon are presented in this section. These results demonstrate that the physical performance of the converter has not been compromised by adapting the prediction horizon, however, there is a significant reduction in the computational cost. The attitude of the output voltage to changes in reference voltage, input voltage and load disturbances are shown.

For the data collection to train the neural network, the range of horizons are $N_{min} = 8$ to $N_{max} = 13$, the output reference voltages are $v_{ref,min} = 20$ V to $v_{ref,max} = 25$ V, the maximum inductor current $i_l = 6$ A and the maximum output voltage $v_o = 26$ V. The value of weighting factor in J_{cp} is $\gamma = 1/2^{N_{max}}$.

The circuit parameters are $C_o = 220$ μF, $L = 450$ μH and $R_l = 0.3$ Ω. The input voltage $v_s = 10$ V and the output reference voltage $v_{ref} = 25$ V. The load resistance is $R = 73$ Ω.

The weighting factor in the objective function (2) is $\lambda = 0.1$, the sampling time interval is $T_s = 5$ μs. For the move-blocking strategy, the parameters are $N_1 = 6$ and $n_s = 4$. As for the Kalman filter, the covariance matrices Q

and R are set as diag([0.1, 0.1, 50, 50]) and diag([1, 1]) respectively.

6.1 Start-Up

The start-up behaviour of the converter under nominal conditions is shown in Fig. 3. It can be seen that the reference output voltage is reached in 2.6 ms without any offshoot. It may also be noticed that during the charging of the inductor, the prediction horizon is adapted to smaller values knowing that a larger prediction horizon would provide no benefit in the performance and hence, reducing the computational cost (cyber utilization). However, when the inductor is charged, the prediction horizon adapts to the maximum value at which the neural network was trained to provide the best possible physical performance. Eventually, when the converter achieves steady-state, the optimal prediction horizon is adapted to track the reference voltage

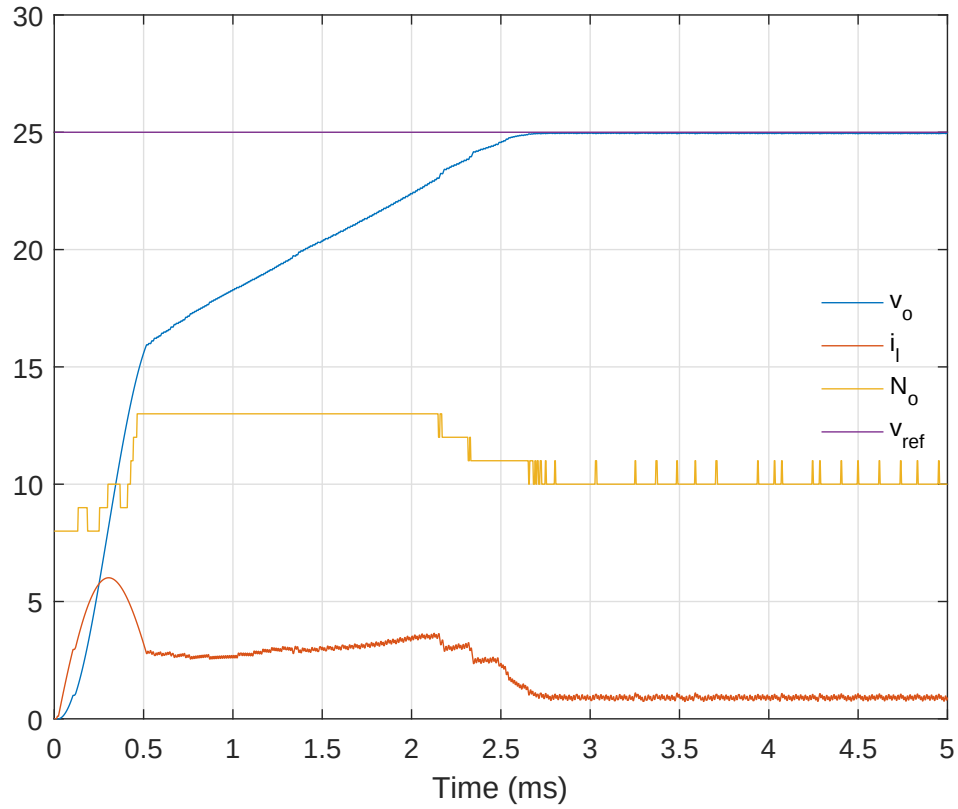

Figure 6.1: A simulated start-up behaviour of output voltage, inductor current and the optimal prediction horizon.

6.2 Step Changes in the Output Reference Voltages

A step-down change in the output reference voltage from 25 V to 20 V was provided at time 1.5 ms as shown in Fig. 4. At the time of transition, a large prediction horizon is desirable to which the prediction horizon adapts and quickly settling for a smaller prediction horizon because in step-down changes, the output capacitor voltage is dropping off and a large prediction

horizon offers no benefit. The inductor current also drops to zero as the capacitor looses its charge. A time of 3 ms is taken for the output voltage to reach the target voltage at which point, the prediction horizon adjusts to the new conditions.

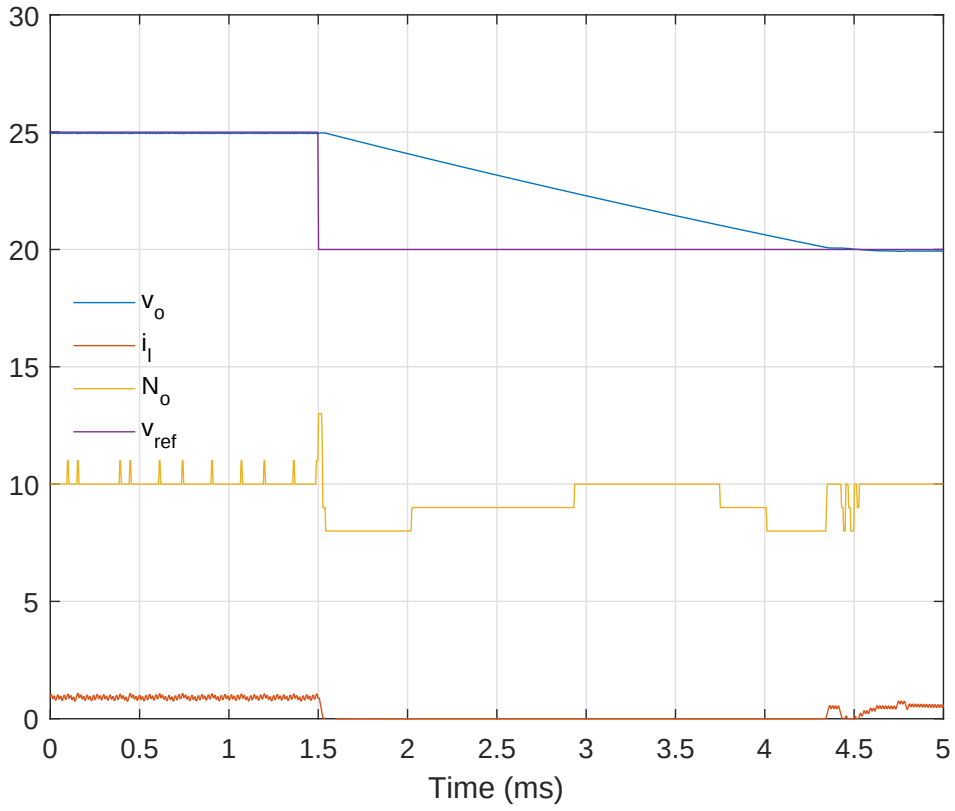

Figure 6.2: The simulated behaviour of output voltage, inductor current and the optimal prediction horizon for a step-down change in output reference voltage.

The behaviour of the output voltage for a step-up change in the output reference voltage is shown in Fig. 5. A step-up change of 5 V was applied which was catered for in about 1.5 ms. At this transition, due to the non-minimum phase behaviour of the boost converter, a large prediction

horizon is required and thus, the prediction horizon adapts and increases to its maximum trained value before falling down to a smaller value once the steady-state is reached.

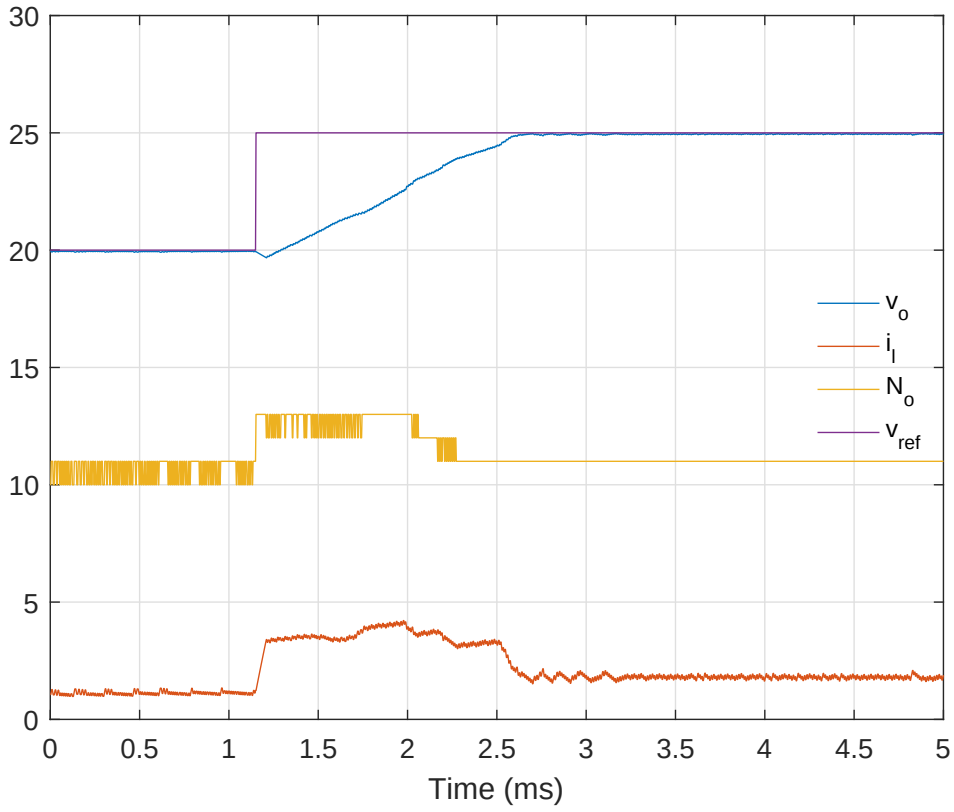

Figure 6.3: The simulated behaviour of output voltage, inductor current and the optimal prediction horizon for a step-up change in output reference voltage.

6.3 Step Change in the Input Voltage

A step change at about 0.58 ms from 10 V to 15 V was applied to the input voltage and the resulting attitude of the output voltage and inductor

current is depicted in Fig. 6 and Fig. 7 respectively. The output voltage is unaffected by this change and as there is no significant change in $v_{o,err}$ and v_o, the prediction horizon is also not affected.

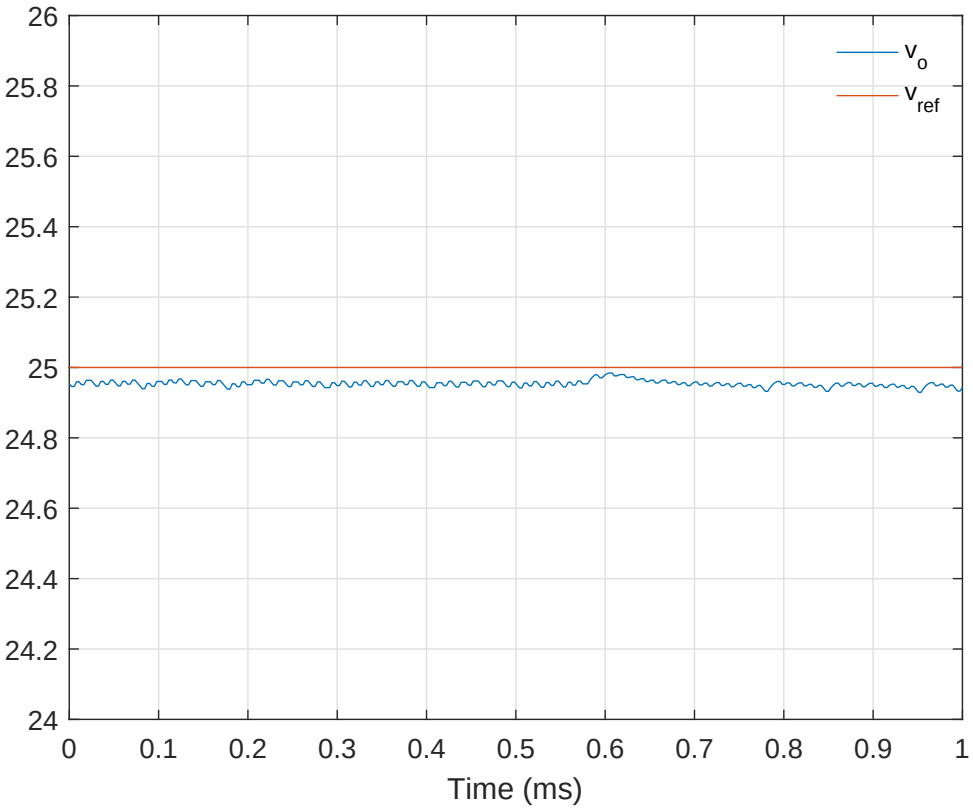

Figure 6.4: The simulated behaviour of output voltage for a step-up change in input voltage.

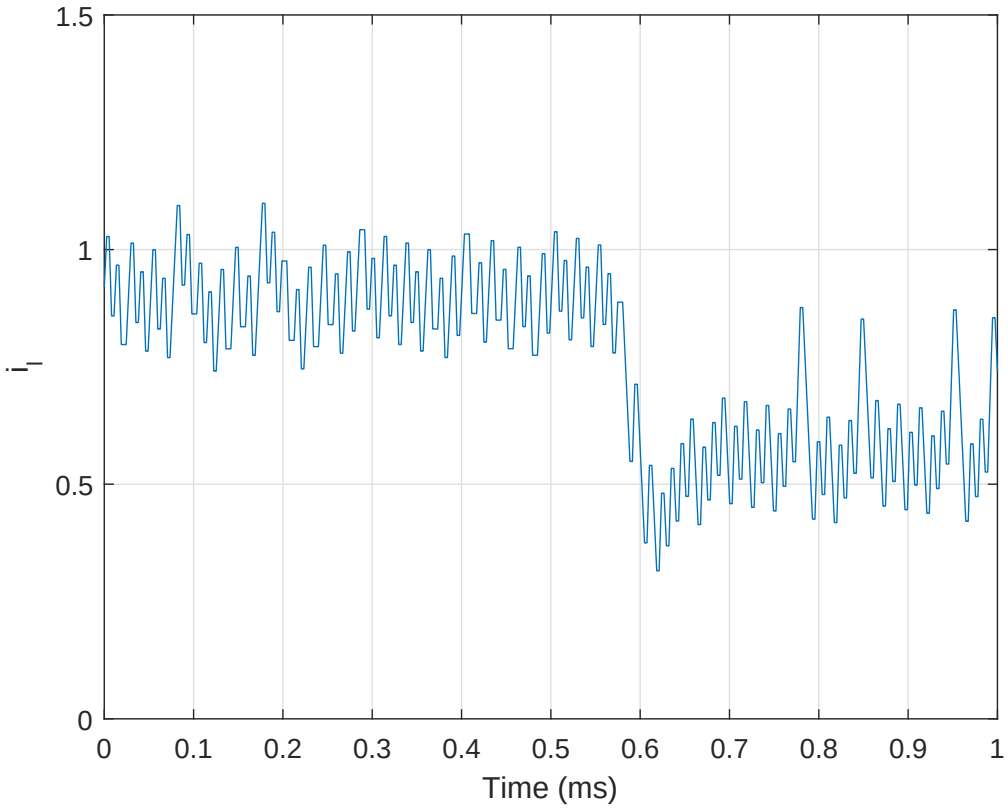

Figure 6.5: The simulated behaviour of inductor current for a step-up change in input voltage.

6.4 Load Step Change

The last case is the change in load. For the converter operating at an input voltage of $v_s = 10$ V and the output reference voltage set at $v_{ref} = 20$ V, the load is changed from $R = 73\ \Omega$ to $R = 36.5\ \Omega$. The behaviour of the output voltage and the prediction horizon is shown in Fig. 8 and 9 respectively. The disturbance in the load occurs at ms. Initially, there is a slight drop in the output voltage during which time the Kalman filter adjusts the reference

output voltage. Once the reference voltage is adjusted to a new value, the output voltage starts creeping up to the desired value. The adjustment in the output reference voltage provides an offset free tracking i.e. no steady-state error. The prediction horizon adapts itself to the changing states of output voltage and the error between the output voltage and the reference voltage as shown in Fig. 9.

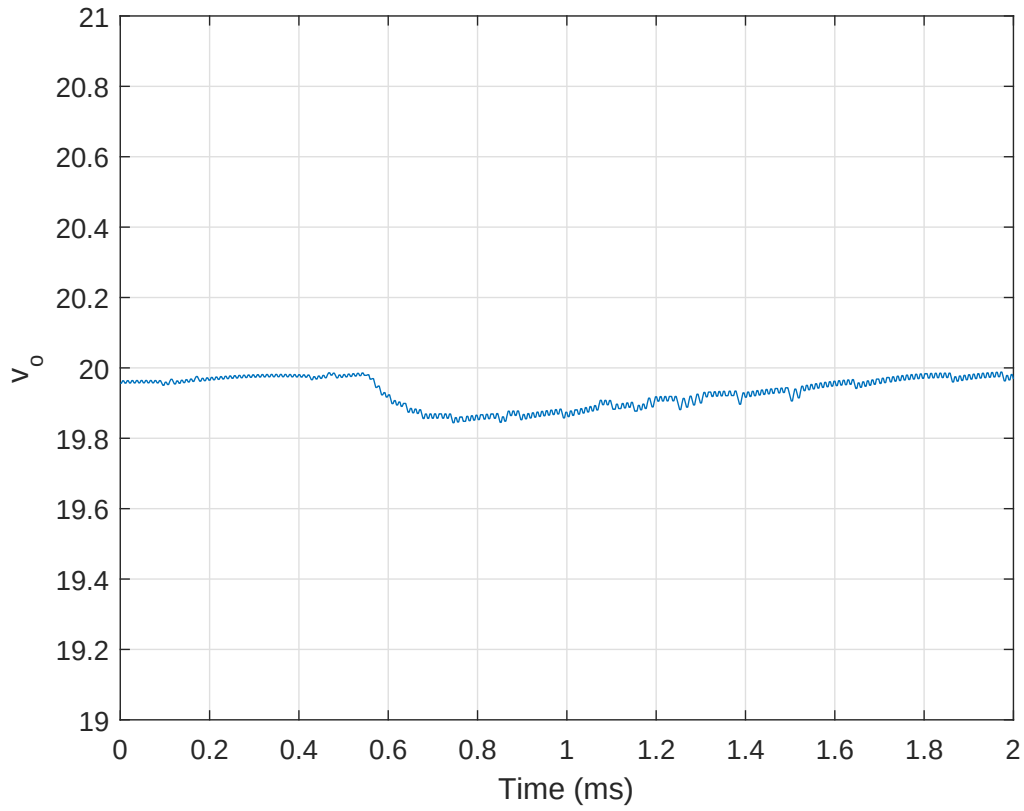

Figure 6.6: The simulated behaviour of output voltage for a change in load.

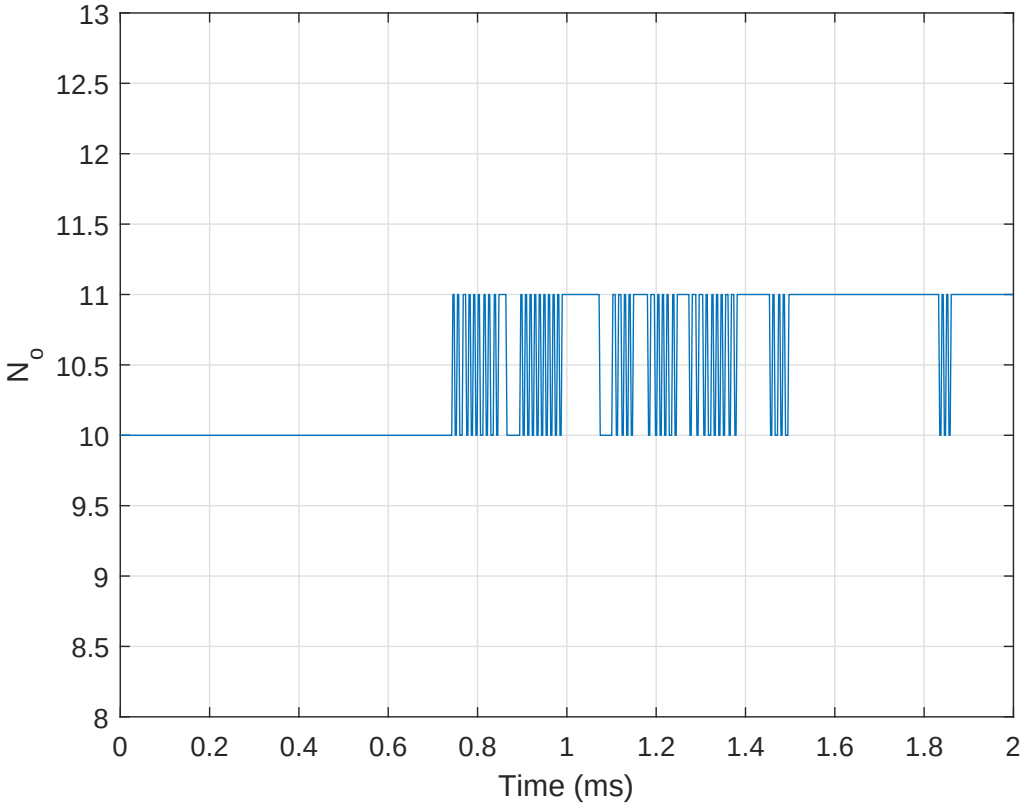

Figure 6.7: The simulated behaviour of the prediction horizon for a change in load.

Chapter 7

Conclusions

During transients and disturbances in the system, a larger prediction horizon N is needed but during the steady state and the initial charging of inductor in boost converter, a smaller prediction horizon is sufficient. In context of this behaviour of the boost converter, a prediction horizon that adapts itself to the state conditions of the converter causes a significant reduction in cyber resources (computational cost) without a compromise in performance. These claims are verified by the results illustrated in chapter 5.

For future works, a method can be developed that varies the value of γ on run-time. This would enable the system to be a true cyber-physical system as we would be able to change the weightage of J_{cp} on run-time. This would enable us to make the system perform physically well or be computationally cost effective. Moreover, for move blocking strategy, the number of prediction steps for fine time steps N_1 is kept constant. We could train a system that varies N_1 as well. by decreasing the value of N_1, the effective prediction horizon increases and vice versa. A trade off for the value of N_1 could also be found to improve the performance of the system while keeping the computational cost at bay.

Bibliography

[1] Justin M. Bradley and Ella M. Atkins. Toward continuous statespace regulation of coupled cyberphysical systems. *Proceedings of the IEEE*, 100(1):60–74, 2012.

[2] Justin M. Bradley and Ella M. Atkins. Coupled cyberphysical system modeling and coregulation of a cubesat. *IEEE Transactions on Robotics*, 31(2):443–456, 2015.

[3] R. W. Erickson and D. Maksimovic. Fundamentals of power electronics. In *2nd ed. Norwell, MA, USA*, 2003.

[4] Tobias Geyer and Daniel E. Quevedo. Multistep finite control set model predictive control for power electronics. *IEEE Transactions on*, 29(12):6836–6846, Dec 2014.

[5] S. Hiti and D. Borojevic. Robust nonlinear control for the boost converter. *IEEE Transactions on Power Electronics*, 10(6):651658, Nov 1995.

[6] G. Espinosa-Perez P. Maya J. Alvares-Ramirez, I. Cervantes and A. Morales. A stable design of pi control for dcdc converters with an rhs zero. *IEEE Transactions on Circuits Systems*, 48(1):103106, Jan 2001.

[7] G. Karsai N. Kottenstette P. Antsaklis V. Gupta B. Goodwine J. Baras J. Sztipanovits, X. Koutsoukos and S. Wang. Toward a science of cyberphysical system integration. *Proceedings of the IEEE*, 100(1):29–44, 2012.

[8] M. K. Kazimierczuk and A. Massarini. Feedforward control dynamic of dc/dc pwm boost converter. *IEEE Transactions on Circuits Systems*, 44(2):143–149, Feb 1997.

[9] M. K. Kazimierczuk and L. A. Starman. Dynamic performance of pwm dc/dc boost converter with input voltage feedforward control. *IEEE Transactions on Circuits Systems*, 46(12):14731481, Dec 1999.

[10] A. Kugi and K. Schlacher. Nonlinear h8 controller design for a dc-dc power converter. *IEEE Transactions on Control Systems Technology*, 7(2):230237, March 1999.

[11] T. M. Undeland N. Mohan and W. P. Robbins. Power electronics: Converters, applications and design. In *3rd ed. Hoboken, NJ, USA*, 2003.

[12] N. Oikonomou F. D. Kieferndorf P. Karamanakos, T. Geyer and S. Manias. Direct model predictive control: A review of strategies that achieve long prediction intervals for power electronics. *IEEE Industrial Electronics Magazine*, 8(1):1894–1905, 2014.

[13] G. Spiazzi P. Mattavelli, L. Rossetto and P. Tenti. General-purpose fuzzy controller for dcdc converters. *IEEE Transactions on Power Electronics*, 12(1):7986, Jan 1997.

[14] L. Rossetto P. Mattavelli and G. Spiazzi. Small-signal analysis of dcdc converters with sliding mode control. *IEEE Transactions on*, 12(1):96102, Jan 1997.

[15] Gabriele Pannocchia and James B. Rawlings. Disturbance models for offset-free model-predictive control. *AIChE Journal*, 49(2):426–437, February 2003.

[16] Tobias Geyer Petros Karamanakos and Stefanos Manias. Direct voltage control of dcdc boost converters using enumeration-based model predictive control. *IEEE Transactions on Power Electronics*, 29(2):968–978, Feb 2014.

[17] E. C. Kerrigan R. Cagienard, P. Grieder and M. Morari. Move blocking strategies in receding horizon control. *Journal of Process Control*, 17(6):563–570, July 2007.

[18] J. B. Rawlings and D. Q. Mayne. Model predictive control: Theory and design. In *Madison, WI, USA*, 2009.

[19] Y. M. Lai S. C. Tan and C. K. Tse. General design issues of sliding-mode controllers in dcdc converters. *IEEE Transactions on Industrial Electronics*, 55(3):11601174, March 2008.

[20] Ren Vargas Ulrich Ammann Samir Kouro, Patricio Corts and Jos Rodrguez. Model predictive controla simple and powerful method to control power converters. *IEEE Transactions on Industrial Electronics*, 56(6):1826–1838, June 2009.

[21] H. J. Sira-Ramirez. Nonlinear p-i controller design for switch mode dc-dc power converters. *IEEE Transactions on Circuits Systems*, 38(4):410417, April 1991.

[22] R. M. Nelms T. Gupta, R. R. Boudreaux and J. Y. Hung. Implementation of a fuzzy controller for dcdc converters using an inexpensive 8-b mi-

crocontroller. *IEEE Transactions on Industrial Electronics*, 44(5):661–669, Oct 1997.

[23] Georgios Papafotiou Tobias Geyer and Manfred Morari. Hybrid model predictive control of the step-down dcdc converter. *IEEE Transactions on COntrol Systems Technology*, 16(6):1112–1124, 2008.

[24] Petros Karamanakos Tobias Geyer and Ralph Kennel. On the benefit of long-horizon direct model predictive control for drives with lc filters. *2014 IEEE Energy Conversion Congress and Exposition (ECCE)*, pages 3520–3527, 2014.